Journal of Power Sources 261 (2014) 337–347

Contents lists available at ScienceDirect

Journal of Power Sources

journal homepage: www.elsevier.com/locate/jpowsour

Battery available power prediction of hybrid electric vehicle based on improved Dynamic Matrix Control algorithms

Limei Wang, Yong Cheng*, Ju Zou

School of Energy & Power Engineering, Shandong University, Jinan 250061, China

HIGHLIGHTS

- A new improved Dynamic Matrix Control algorithm is proposed.
- The method can be used to predict battery voltage and available power dynamically.
- A single RC block model is adequate for the dynamic characteristics of a battery.
- Bench and HEV tests are performed to verify the validity of the algorithm.
- A fixed time constant can also achieve satisfactory results in the algorithm.

ARTICLE INFO

Article history:
Received 24 November 2013
Received in revised form
7 January 2014
Accepted 20 March 2014
Available online 27 March 2014

Keywords:
Original Dynamic Matrix Control algorithm
Identification
Prediction
Available power
Hybrid electric vehicle

ABSTRACT

The core technology to any hybrid engine vehicle (HEV) is the design of energy management strategy (EMS). To develop a reasonable EMS, it is necessary to monitor the state of capacity, state of health and instantaneous available power of battery packs. A new method that linearizes RC equivalent circuit model and predicts battery available power according to original Dynamic Matrix Control algorithm is proposed. To verify the validity of the new algorithm, a bench test with lithium-ion battery cell and a HEV test with lithium-ion battery packs are carried out. The bench test results indicate that a single RC block equivalent circuit model could be used to describe the dynamic and the steady state characteristics of a battery under testing conditions. However, lacking of long time constant of RC modules, there is a sample deviation in the open-circuit voltage identified and that measured. The HEV testing results show that the battery voltage predicted is in good agreement with that measured, the maximum difference is within 3.7%. Fixing the time constant to a numeric value, satisfactory results can still be achieved. After setting a battery discharge cut-off voltage, the instantaneous available power of the battery can be predicted.

1. Introduction

Taking full advantage of the motor and the engine, a hybrid engine vehicle (HEV) can work well at high efficiency. Hybrid technology is considered one of the most promising technologies in the future of the automobile. The core technique to any successful HEV is the design of the vehicle energy management strategy. A reasonable energy management strategy can fully exploit the advantages of the engine and the motor to achieve good energy conservation and emissions reduction [1].

To develop a reasonable energy management strategy, the state of charge (SOC), the state of health (SOH) and the instantaneous available power of battery packs should be monitored [2,3]. Among these values used to describe the present state of the battery packs, more precisely SOC estimation would guarantee the HEV working in the higher efficiency range and slow the aging of the battery packs.

Many algorithms have been proposed in the literature for the SOC estimation and other related problems. Some basic algorithms used for the SOC estimation were summarized, and their characteristics and application ranges were comparatively analyzed [3].

Generally, standard current integration method combined with open circuit voltage [4], Kalman filters [5,6], or sliding mode observers [7] methods are used to estimate the SOC in vehicle applications, and have error that could be less than 5%. As the SOC plays a major role in the SOH determination, the SOH can be

* Corresponding author.
E-mail address: cysgd@sdu.edu.cn (Y. Cheng).

http://dx.doi.org/10.1016/j.jpowsour.2014.03.091
0378-7753/

predicted conveniently once the SOC has been determined accurately. For example the Dual-Kalman filter method is a very promising method to estimate the SOH based on the SOC [8].

The main difficulty in predicting remaining available power is that the battery parameters are influenced by battery age, operation mode and the work environment. Therefore, the estimation accuracy of remaining available power relies not only on the reliability of the battery model, but also on the accuracy of the model parameters determination [9].

Model parameters can be identified online or offline. The offline method estimates the battery state parameters according to a pre-calibrated map in a laboratory. The map presents the relationship among model parameters, such as current and temperature as well as SOC. This method is implemented in the ADVISOR application, for example.

As reported in previous literature, the battery model parameters are impacted by battery age, operation mode and work environment [10]. Furthermore, the parameters of battery cells that are from the same batch of a manufacturer have some differences [11]. So, online parameter identification is particularly important to an operating vehicle.

Plett proposed a method that identified parameters of a battery cell and estimated battery SOC, SOH and pack available dis/charge power dynamically by the Kalman filter method [12]. Li achieved online parameter identification of a second RC block equivalent circuit model using the least squares method [13]. Xing developed the 'ensemble' model to characterize the capacity degradation and predict the remaining useful performance. The parameters of the model were adjusted online based on the particle filter algorithm approach [9]. Y. Hu linearized a second RC block equivalent circuit model using the linear spline functions and subspace methods respectively, and identified the model parameters by the genetic algorithm [1,14].

The original Dynamic Matrix Control (DMC) algorithm is applied in a wide range of control engineering applications. It refers to a class of advanced control algorithms that compute a sequence of manipulated variables in order to optimize the future behavior of the controlled process and is suitable for predicting the future behavior of a model [15]. To simplify the identification of battery model parameters, a new approach to linearize RC block equivalent circuit models using the original DMC algorithm is proposed. Furthermore, a new method taking advantage of the predictive features of the original DMC algorithm to predict battery available power is discussed in this paper.

2. Battery model

The commonly used battery models are electrochemical models and equivalent circuit-based models. Electrochemical models are based on the battery physical construction and chemistry. They usually have high accuracy in predicting the output behavior of the battery since they accurately describe the fundamental mechanism of battery power generation. Such models typically contain systems of coupled partial differential equations that are difficult to simulate or solve and generally are not suitable for a control system [1]. As a compromise between accuracy and usability, the equivalent circuit-based models are often adopted. These models approximate the underlying dynamics with an equivalent circuit which is are often much simpler in structure thus making them suitable for onboard computation.

Typical equivalent circuit models include Rint model [16], RC model [17], Thevenin model [18] and PNGV model [19]. To describe a lithium-ion battery, an n-RC blocks equivalent circuit model with no parasitic branch is a common choice [20]. Fig. 1 shows an n-RC blocks equivalent circuit model.

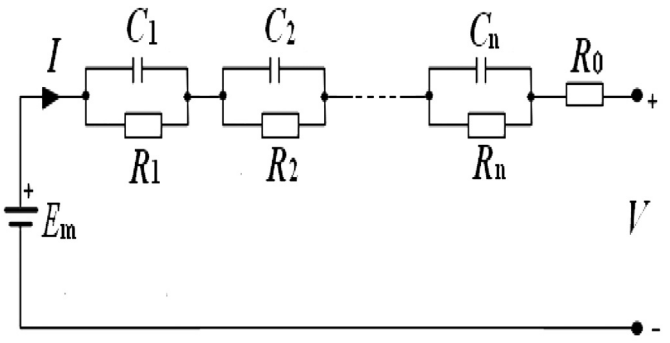

Fig. 1. n-RC blocks equivalent circuit model.

In Fig. 1, E_m represents the open circuit voltage which is related to the battery SOC and temperature. R_0 is the ohmic internal resistance, R_i and C_i represents polarization resistance and capacitance respectively, $i = 1,2, \ldots, n$, which are used to simulate the different concentration polarization and electrochemical polarization dynamic characteristics of a battery. I is the battery current, V denotes the battery voltage output. All R_0, R_i and C_i are functions of the battery SOC, temperature and current.

Battery voltage output V is found by Kirchhoff's voltage law:

$$V = E_m - V_{R_0} - \sum_{i=1}^{n} V_{R_i} \tag{1}$$

where, V_{R_0} is the voltage across the ohmic internal resistance R_0, V_{R_i} represents the voltage across each R_iC_i circuit segment.

Each R_iC_i circuit could be described by an ordinary differential equation deduced by Kirchhoff's current law:

$$\frac{dV_{R_i}}{dt} = -\frac{V_{R_i}}{C_iR_i} + \frac{1}{C_i}I \tag{2}$$

Equation (2) can be reformulated as:

$$V_{R_i} = IR_i\left(1 - e^{-t/R_iC_i}\right) \tag{3}$$

Thus, the battery voltage output V can be expressed as:

$$V = E_m - V_{R_0} - \sum_{i=1}^{n} IR_i\left(1 - e^{-t/R_iC_i}\right) \tag{4}$$

3. DMC identification and predication algorithm

3.1. Principle of DMC identification and predication algorithm

DMC algorithm is a predictive control algorithm based on step response. The linear step response model used by the DMC algorithm relates to changes in a process output to a weighted sum of past input changes, referred to as input movements. By using the step response model, we can control predicted future output changes as a linear combination of future input movements [15]. Thus, the circuit segment can be described by a dynamic matrix $A_i = (a_{i1}, a_{i2}, \ldots, a_{iN})$, where a_{ij} is the j-th step response coefficient for the i-th circuit segment, N_i is the length of output stability for the i-th circuit segment. The battery output voltage can be calculated as follows at k time.

$$V_k = E_m - I_kR_o - \sum_{i=1}^{n} R_i\left(I_{k-N_i} + \sum_{j=1}^{N_i}\left(I_{k-j} - I_{k-j-1}\right)a_{ij}\right) \tag{5}$$

Model parameters identification method is as follows, selecting an appropriate length of matrix or time constant to describe the R_iC_i module, the model parameters finally can be solved with the least squares method. By means of the measured battery current and voltage, the variables in equation (5) can be solved by using the constraint

$$Q\left(E_m^*, R_0^*, R_i^*\right) = \min Q(E_m, R_o, R_i)$$

where, $Q=\sum_{k=1}^{M}(V_k-E_m+I_kR_o+\sum_{i=1}^{n}R_i(I_{k-N_i}+\sum_{j=1}^{N}a_{ij}(I_{k-j}-i_{k-j-1})))^2$

By solving $\partial Q/\partial R_i = 0$, $\partial Q/\partial E_m = 0$, $\partial Q/\partial R_0 = 0$ to minimize the solution of $Q(E_m, R_0, R_i)$. Then, E_m^*, R_0^*, R_i^* can be found.

3.2. Prediction results and validation

In order to verify the validity of the algorithm, experiments are carried out at a test bench. The test bench comprises a constant temperature and humidity test chamber and a battery performance tester. The specifications of the major equipment are shown in Table 1.

Eight battery cells are used to carry out discharge tests simultaneously under 5 °C, 25 °C and 45 °C respectively. For preparation, each battery capacity is measured under testing temperature according to '2008 EV lithium-ion power battery test specification'. In which, a full charged battery is discharged at C/3 (1/3 times of battery capacity) until the battery voltage reaches the low voltage limit and then its capacity is measured.

A curve segment for discharge current control is shown in Fig. 2. The current curve refers to a segment of real vehicle collection data and the current is scaled down proportionally for limiting the maximum current to 50 A to suit for the battery performance tester. The segment lasts 1072 s and discharges 4.5 Ah correspondingly. Repeating 3 times is termed a testing cycle, and total discharges 13.45 Ah in a cycle. At least 5 h rest is inserted between successive cycles, and the cycle will be repeated till the battery cell voltage decreases to the end of discharge voltage. And then, each battery cell's remaining capacity is measured again. The battery voltage, current and temperature are recorded every 0.2 s.

The experimental results are basically similar at 5 °C, 25 °C and 45 °C, therefore, the discussion examples in this paper will use the results taken at 25 °C.

The testing process contains seven discharge cycles, the first six cycle test results are basically similar. Fig. 3(a), (b) shows the test results of No. 1 battery cell at first and seventh cycle respectively, the rest of battery cells test results are consistent with these basic results.

The capacity of No. 1 battery cell is 95.63 Ah. The SOC drops from 100% to 86% in the first cycle, and the open circuit voltage is 3.334 V after 5 h rest. The SOC changes from 14% to 0.6% in the seventh cycle.

As shown in Fig. 3, the battery voltage follows the current. When the current stops, the battery voltage will recover rapidly at first and then follow a smooth recovery phase. A second RC block model

Table 1
Specifications of major equipment.

Item	Model	Characteristics
Constant temperature and humidity test chamber	BE-TH-225L8	Temperature: −70 °C–150 °C (±1 °C); humidity: 20%–98%
Battery performance tester	BTS550C8	8 channels; voltage: 0–5 V (0.1% FS); Current: 150 mA–50 A (0.1% FS)
Lithium-ion battery	JL-100 Ah	Capacity: 100 Ah; rated voltage: 3.2 V

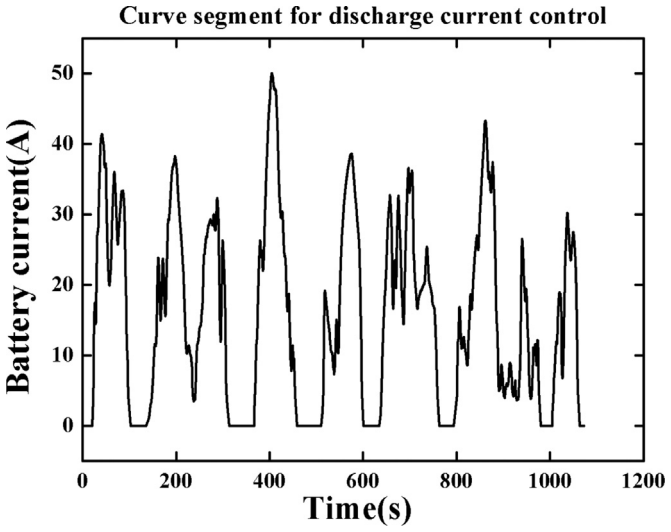

Fig. 2. Curve segment for discharge current control.

is used to fit the voltage recovery curve. The results indicate that the fitting curve with time constants of 200 s and 3000 s respectively will agree well with the testing result, just as shown in Fig. 4. This supposes that the influence of long time constant RC blocks is not

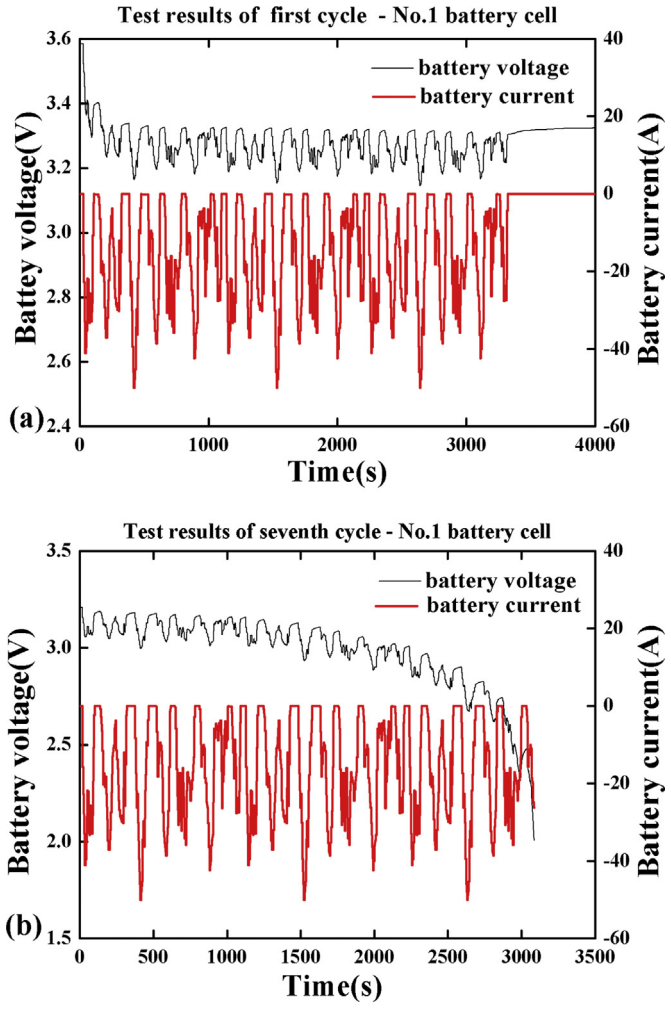

Fig. 3. Test results of No. 1 battery cell at first and seventh cycle.

significant when the current changes drastically. The more severely the current changes, the more significant is the shorter time constant effect.

Li pointed out that the voltage response time was above several tens of seconds, even over several minutes for a lithium-ion battery [21]. Statistical results indicate that the shorter time constant is between 10 s and 50 s. The time constants range between 10 s to 50 s and 150 s to 250 s for a second RC block equivalent circuit model are chosen to identify the model parameters. Because the battery parameters are assumed to be constant in model parameters identifying and battery output state predicting, the period for model parameter identification should be chosen as short as possible. Balancing computation workload and prediction accuracy, 100 s of test data is selected for model parameter identification. Based on the parameters obtained from the identification, the voltage in the next 10 s is predicted using the measured current. The forecasting process is repeated at 10 s step interval. Figs. 5 and 6 compare the results of measured and predicted battery voltage as well as their difference. The curves are corresponded to No. 1 battery cell at the first cycle. Fig. 5 shows that the predicted voltage coinciding well with the measured voltage. Fig. 6 shows that the maximum difference between the predicted and the measured voltage is not more than 0.004 V along the whole curve. In order to reduce the computation workload, the identification and the prediction process are also carried by a first RC block equivalent circuit model with time constant in 10–50 s and the results are shown in Figs. 7 and 8. Figs. 7 and 8 show that the first block RC equivalent circuit model reaches similar results to the second RC block equivalent circuit model. In other words, both models could predict battery voltage with similar accuracy. Therefore, the first block RC equivalent circuit model is selected for the subsequent discussion.

As a contrasting, the battery voltage is also evaluated by the extended Kalman filtering algorithm combined with the recursive least square (RLS) algorithm. The results are shown in Figs. 9 and 10. Comparing Fig. 8 with Fig. 10 shows that the battery voltage predicting accuracy with 'DMC identification and prediction' algorithm is some lower than that with the extended Kalman filtering algorithm. This phenomenon can be attributed to that the 'DMC identification and prediction' algorithm predicts the battery voltage in the next 10 s using the past measured data, and the battery parameters have some changed in the process. In contrasting, the extended Kalman filtering algorithm evaluates the battery voltage based on the battery parameters with the same moment.

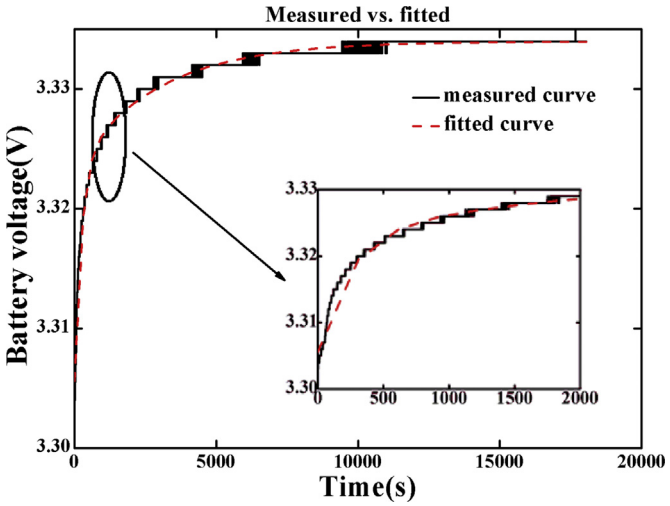

Fig. 4. Fitted voltage curve against the measured based on a second RC block model.

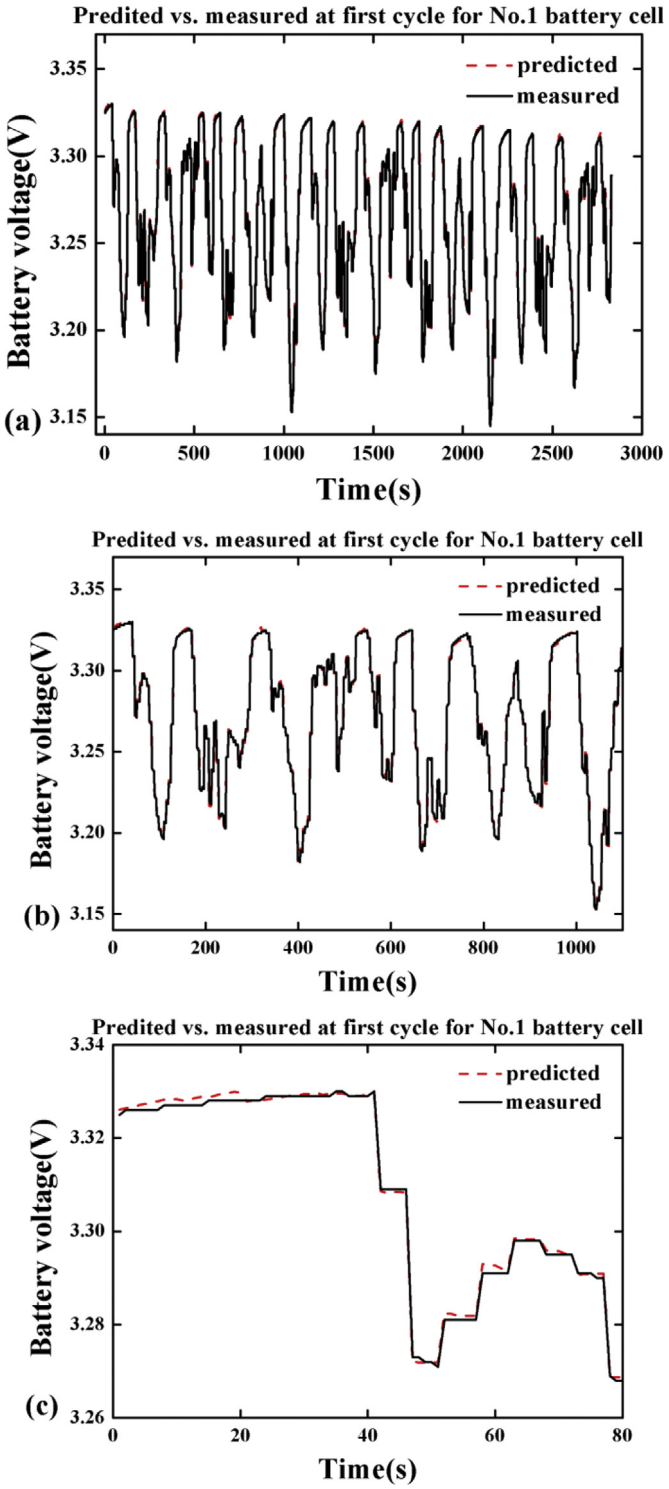

Fig. 5. Results of measured and predicted with different time sizes at first cycle for No. 1 battery cell based on a second RC block model.

The validation of this method is based on the suppose that the battery parameters are nearly unchanged in the identification and prediction process, otherwise a large deviation will occur. Figs. 11 and 12 give predictive results for the seventh cycle. Fig. 12 shows that a 0.35 V deviation appears near the end of the cycle. At that time, the battery remaining capacity is about 0.65 Ah with 0.68% SOC, and the battery cell parameters are changing rapidly.

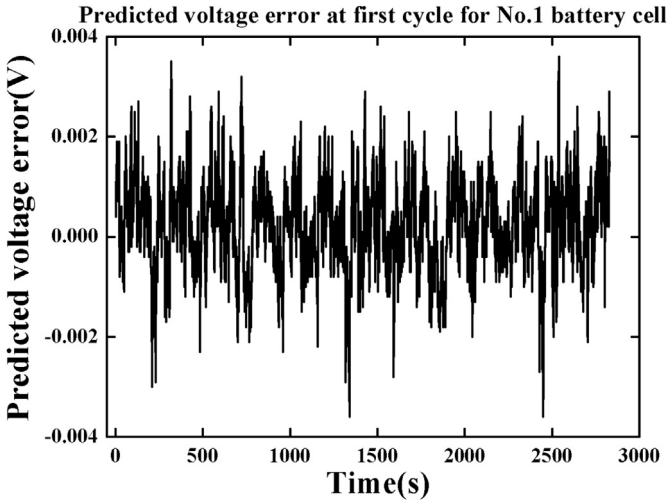

Fig. 6. Predicted voltage error at first cycle for No. 1 battery cell based on a second RC block model.

Fig. 13 shows the open circuit voltage and battery ohmic internal resistance curve identified in the first cycle. It can be seen from Fig. 13(a) that the battery open circuit voltage curve is in decline generally with the discharge process and this trend is consistent with the experience. The averaging battery ohmic internal resistance is 3.13 mΩ in Fig. 13(b). The 'Freedom CAR Battery Test Manual for Power-Assist Hybrid Electric Vehicles' suggests estimating the ohmic internal resistance of battery with $\Delta U/\Delta I$. Furthermore, it indicates that when battery ohmic internal resistance is small, the discharge current should be at least 5 C [19]. At the cycle start instant, with a steep current changing of 15.8 A (0.16 C), the ohmic internal resistance of battery is extracted and the value is about 3.04 mΩ. There is about 0.09 mΩ difference between that from identification (by 'DMC identification and predication' algorithm) and calculation (by equation). The difference is supposed to be impacted by the limitation of the first RC block equivalent circuit. The equation (5) shows that the first RC block equivalent circuit has omitted some of the polarization resistances which are generally described by long time constant RC blocks. Therefore, the identified ohmic internal resistance inevitably contains some polarization resistances. However, considering actual applications, it indicates that the parameter identification method according to 'DMC identification and prediction' algorithm is valid and useful.

The proposed prediction method based on 'DMC identification and prediction' algorithm predict battery voltage according to the current step response. The identification window is determined by the length of the dynamic matrix A, in other words, the maximum prediction length in the rest stage is the length of the dynamic matrix A after the battery load stops. Fig. 14(a) shows the difference between measured and predicted voltage of No. 1 battery cell at the end point of each predicting cycle. This figure indicates that within the scope of the 'DMC identification and prediction' algorithm, the maximum predicting voltage deviation is about 0.002 V ± 0.001 V. Fig. 14(b) compares the identified open circuit voltage with that measured from battery rest of No. 1 for each cycle, the maximum difference is about 0.024 V ± 0.001 V. With reference to Fig. 3(a), it is supposed that the difference is also due to the lack of long time constants in RC blocks.

The 'Hybrid Pulse Power Characterization' (HPPC) method [22] is commonly used to calculate the available power from a cell during cell testing. Maximum current is computed using a simple cell model, ensuring that the cell's terminal voltage remains within limits, and power is computed by multiplying cell current by cell voltage. Pack power is calculated by multiplying the minimum cell power by the number of cells in the pack.

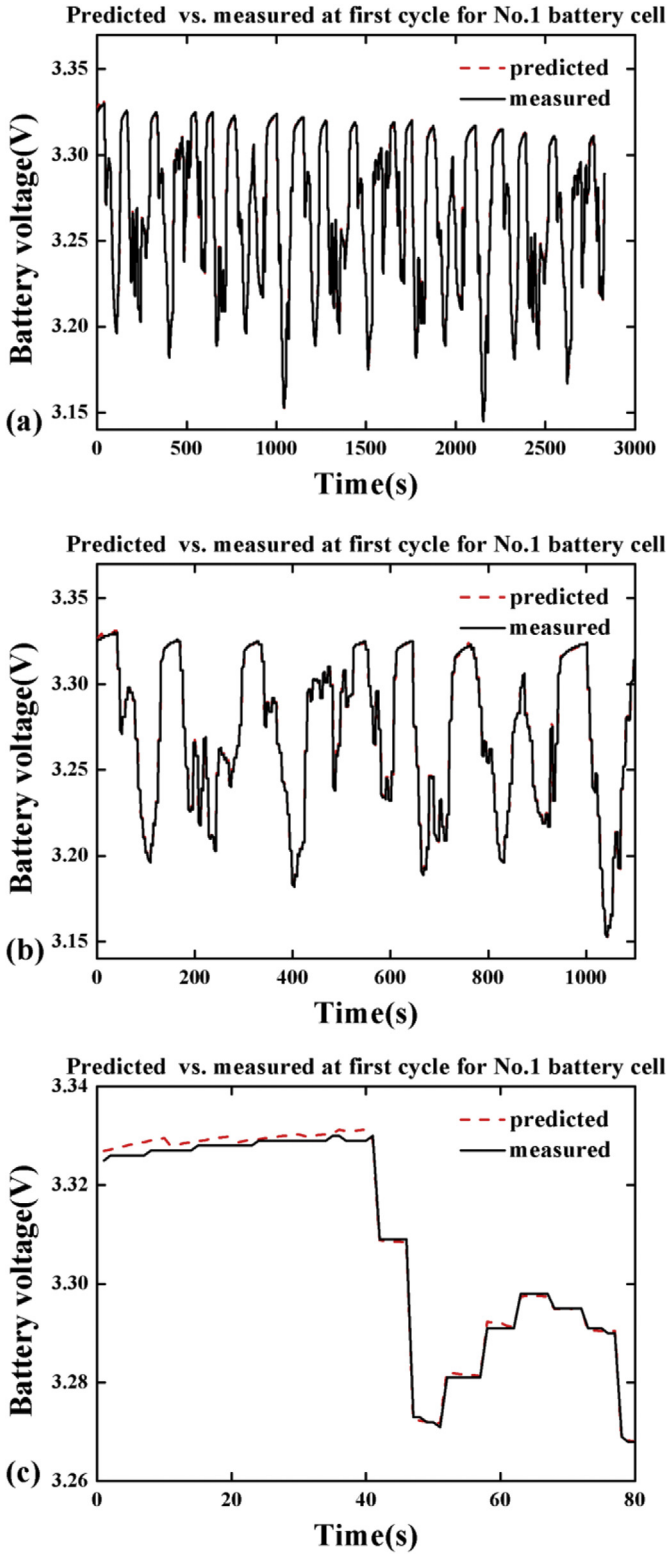

Fig. 7. Results of measured and predicted with different time sizes at first cycle for No. 1 battery cell based on a first RC block model.

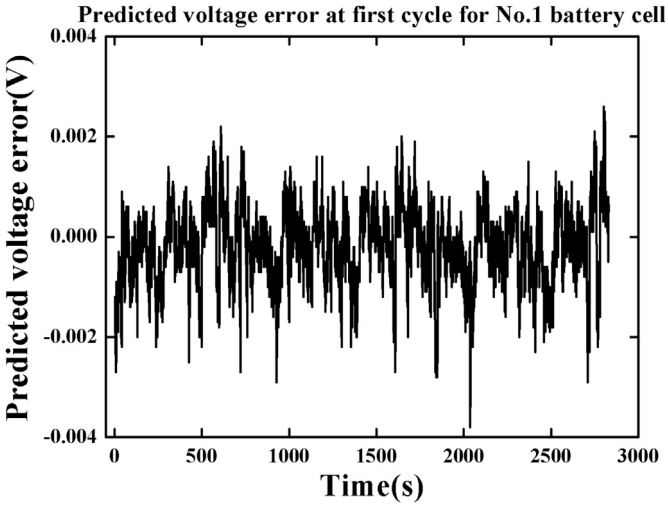

Fig. 8. Predicted voltage error at first cycle for No. 1 battery cell based on a first RC block model.

Given the battery parameters identified and the end of discharge voltage permitted, the maximum continuous discharge current in the future time (Δt seconds) can be calculated by 'DMC identification and prediction' algorithm. The discharge power available at this time is determined by equation (6),

$$P = U_{\text{limit}} I_{\text{max}} \tag{6}$$

where, P is the discharge available power, U_{limit} represents the permitted end of discharge voltage, I_{max} is the continuous discharge current in the discharge time Δt seconds.

Tests have been carried out to verify the accuracy of available power estimation. These tests are not designed to predict the maximum continuous discharge current based on discharge cut-off voltage directly, but make use of the maximum discharge current (50 A) of battery performance tester as the discharge current. The test cycle has 2 stages, first—discharge according to Fig. 2, then second—apply a 50 A continuous discharge for 60 s. Based on the battery parameters identified at the first stage, the battery voltage at the next stage is predicted. The difference between the predicted and measured battery voltage is used to evaluate the available power prediction accurately. The test consisted of 16 cycles until the discharge voltage went down to 2.5 V. Fig. 15 shows the relative error of the predicted voltage and the measured voltage at the end of the second stage. It can be seen from the figure, the maximum error is within 0.04%.

The tests for the battery cell (3.65 V, 100 Ah) are limited by the battery performance tester, the maximum current is setted to 50 A or 0.5 C. A smaller capacity battery cell (3.65 V, 10 Ah) is also used to perform a test. At this time, the maximum current is setted to 20 A or 2 C. The test cycle also has 2 stages, discharging according to Fig. 2 and applying a 20 A continuous discharge for 60 s. The testing results are shown in Fig. 16. Fig. 17 compares the measured and the predicted battery voltage as well as their difference. Fig. 17(b) shows that the maximum error is within 0.2%.

A constant current discharge test is also carried out with the smaller battery cell. The testing results are shown in Fig. 18. Fig. 19 compares the measured and the predicted battery voltage as well as their difference. Fig. 19(b) shows that the maximum error is within 0.2% under the constant discharge condition, and a 0.01 V deviation appears near the end of the cycle. At that time, the battery remaining capacity is about 0.71 Ah or 0.7% SOC, and the battery cell parameters are changing rapidly.

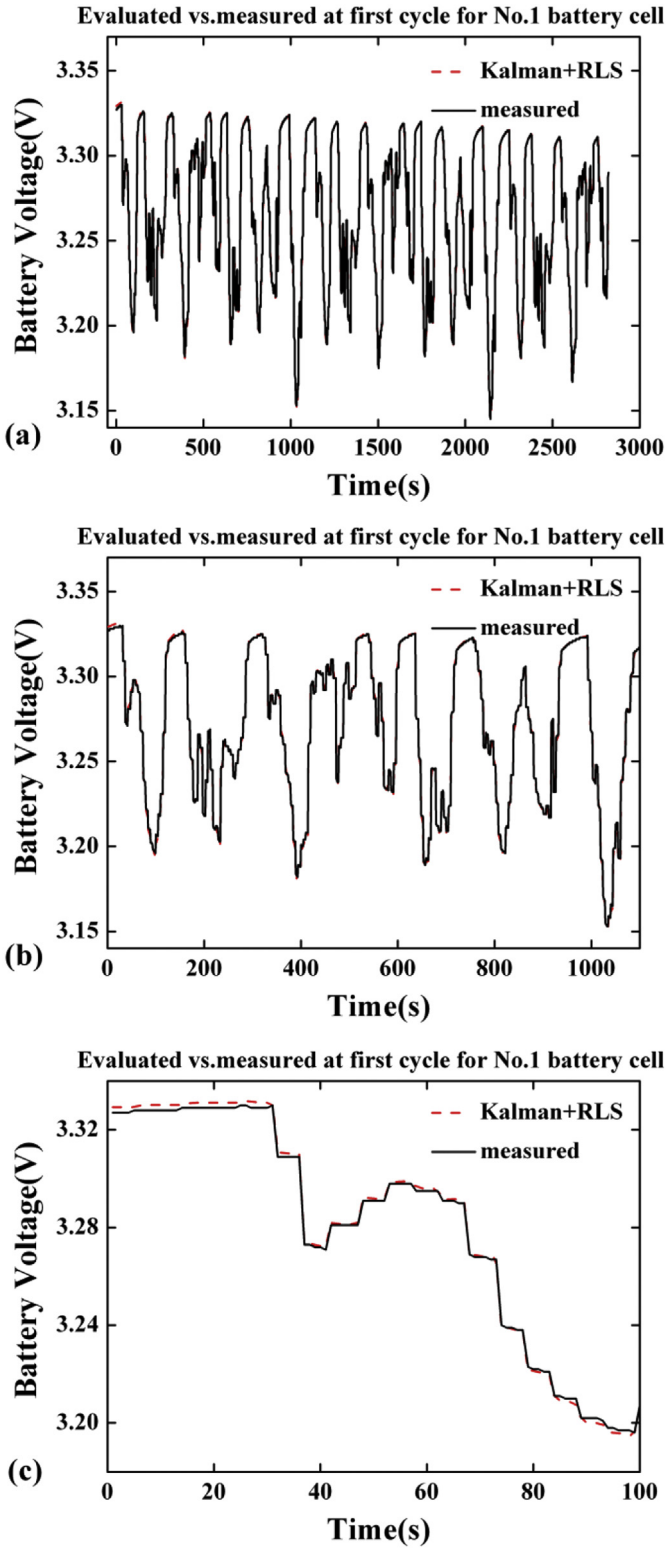

Fig. 9. Results of measured and evaluated with different time sizes at first cycle for No. 1 battery cell based on a first RC block model by Kalman filtering algorithm.

4. HEV validation

Fig. 20 shows a set of battery voltages and current curves measured on a HEV. The vehicle is equipped with lithium-ion battery packs (320 V, 66 Ah).

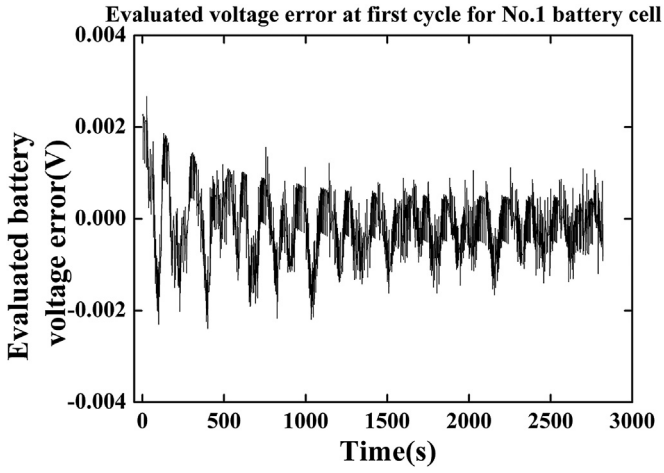

Fig. 10. Evaluated voltage error at first cycle for No. 1 battery cell based on a first RC block model by Kalman filtering algorithm.

Figs. 21 and 22 show the predicted and the measured battery voltages as well as the difference between them. As can be seen, the voltage predicted by 'DMC identification and prediction' algorithm is in good agreement with that measured, the maximum difference

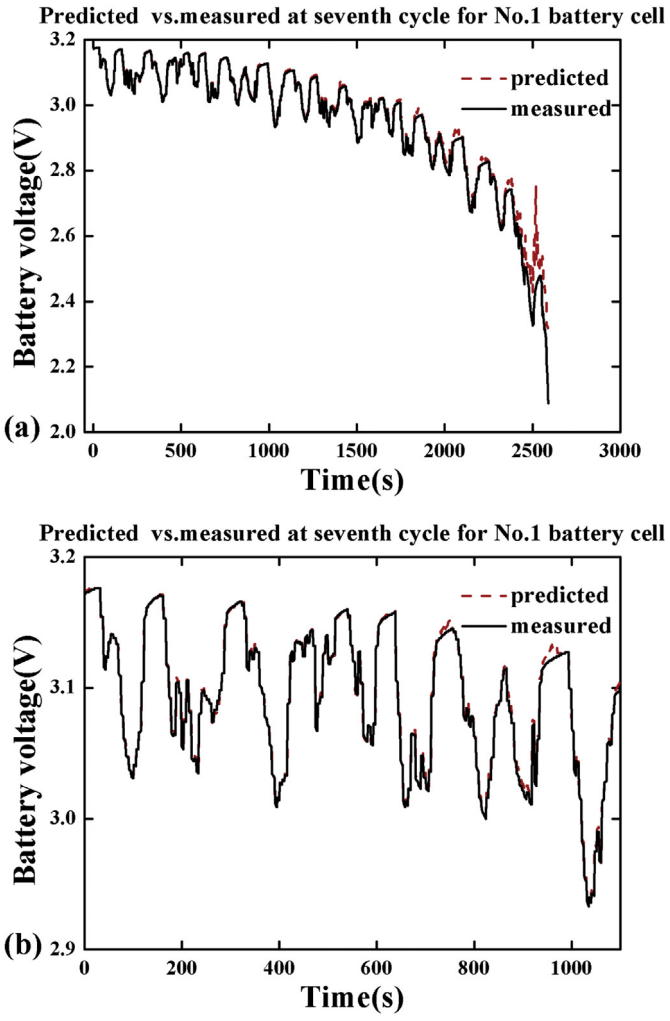

Fig. 11. Results of measured and predicted with different time sizes at seventh cycle for No. 1 battery cell based on a first RC block model.

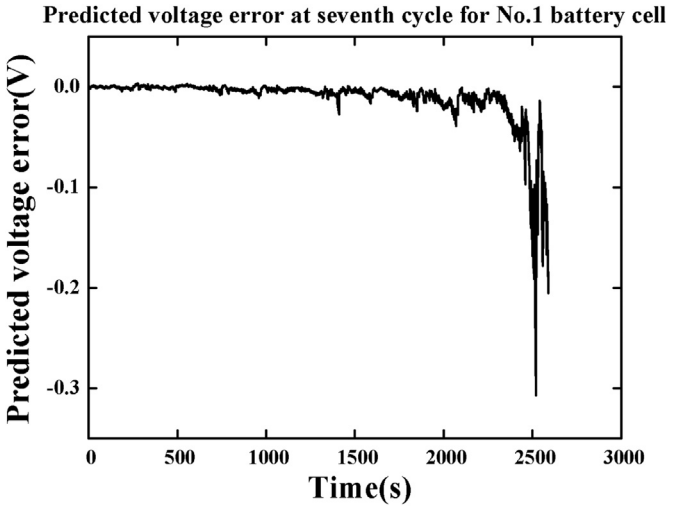

Fig. 12. Predicted voltage error at seventh cycle for No. 1 battery cell based on a first RC block model.

is within 3.7%. Reference to Fig. 20(a), some battery current beyond the current sensor range under energy feedback condition, the negative maximum current is cut to −100 A. The phenomenon prompts a large deviation of predicted results. It is concluded that the battery voltage could be predicted accurately based on the 'DMC identification and prediction' algorithm and the measured

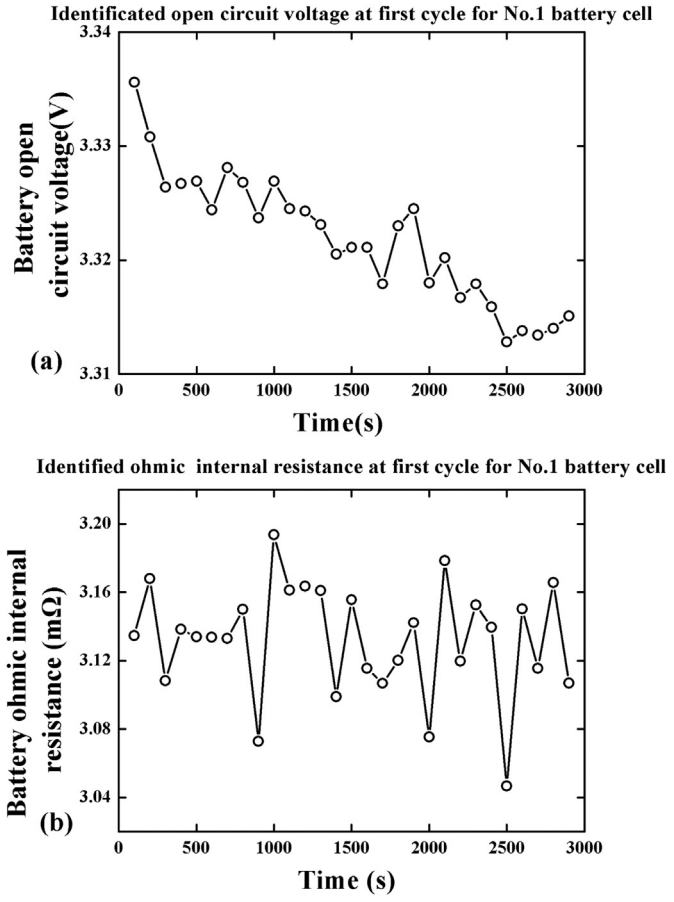

Fig. 13. Identified battery parameters at first cycle for No. 1 battery cell based on a first RC block model.

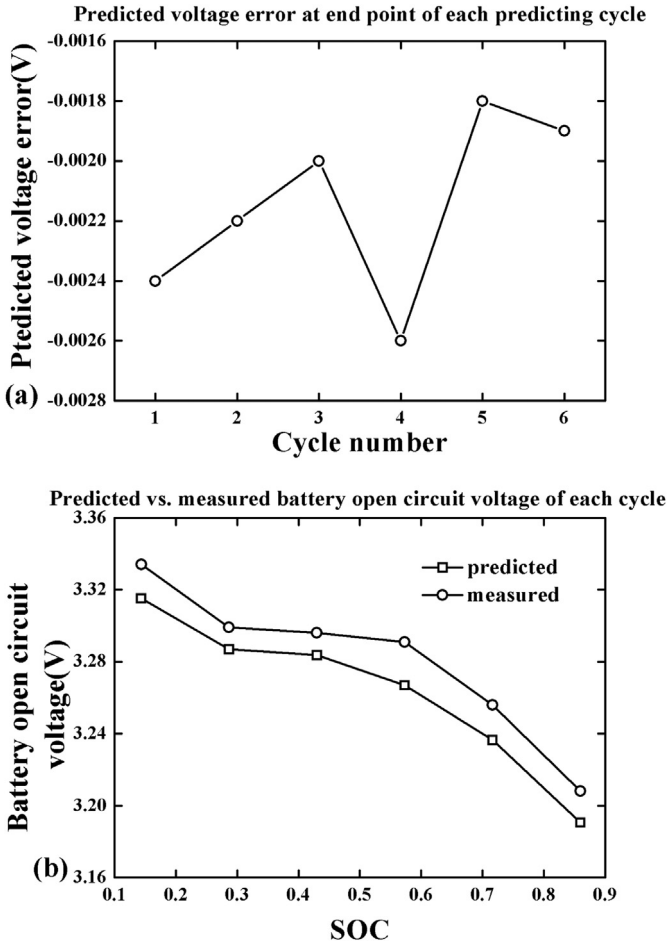

Fig. 14. (a) Predicted battery voltage error at end point of each predicting cycle and (b) predicted vs. measured battery open circuit voltage for each cycle of No. 1 battery cell based on proposed prediction method.

current. By setting the end of discharge voltage, battery available power could also be predicted.

In order to reduce the computation workload and simplify the application for a battery management system (BMS), a fixed time

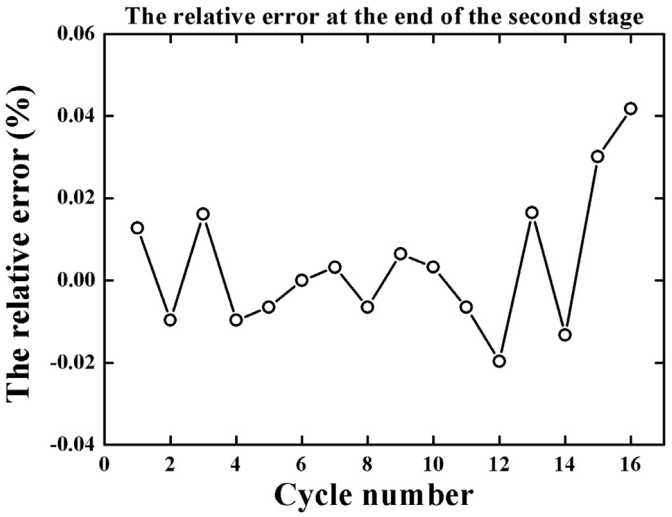

Fig. 15. The relative error of the predicted and measured at the end of each second stage of No. 1 battery cell.

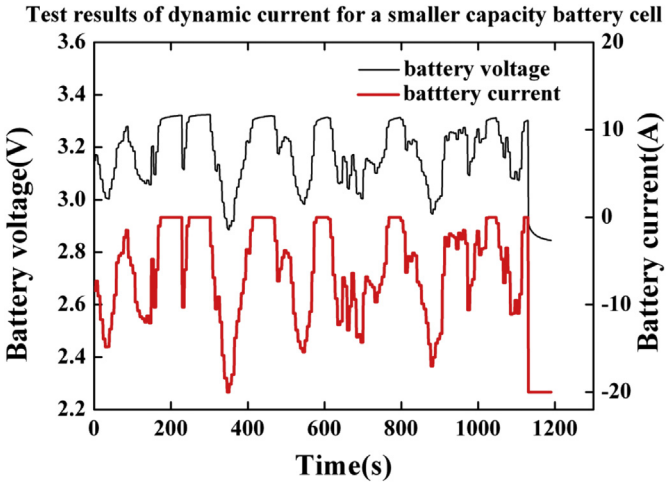

Fig. 16. Test results of dynamic current for a smaller capacity battery cell.

constant is used and the corresponding prediction accuracy is discussed. The identification and prediction process as in Figs. 21 and 22 are repeated using a fixed time constant 25 s, the results are shown in Fig. 23 and 24. Statistical analysis of the data in

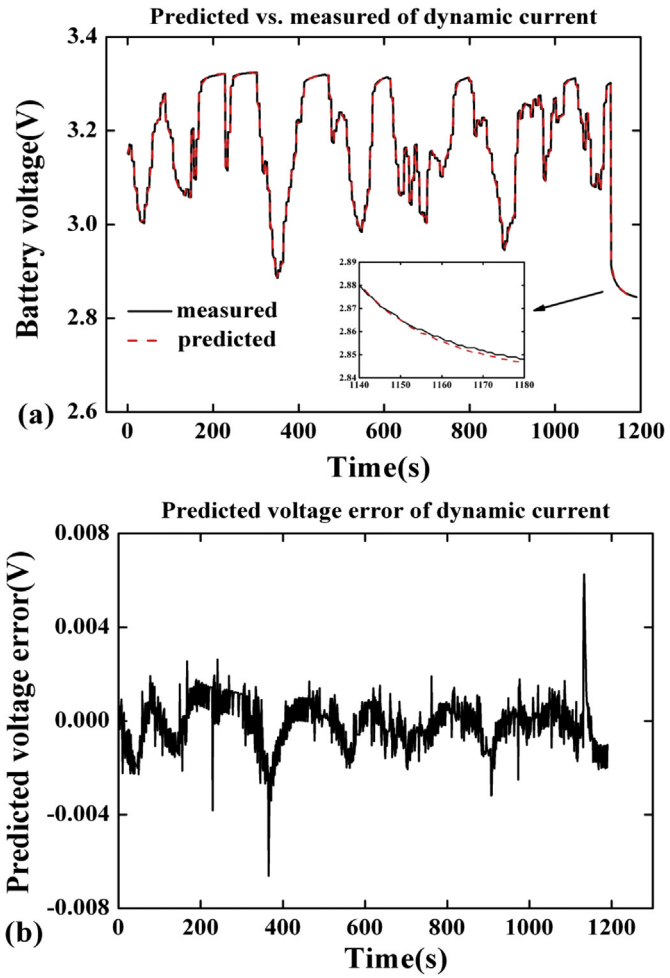

Fig. 17. (a) Results of measured and predicted with different time sizes of dynamic current for a smaller capacity battery cell and (b) predicted voltage error of dynamic current for a smaller capacity battery cell.

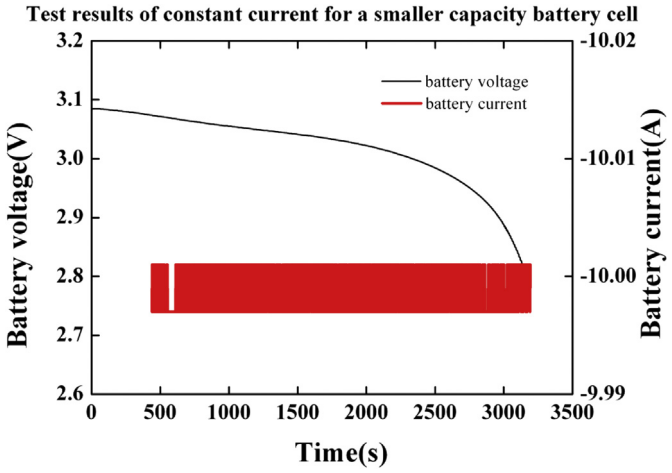

Fig. 18. Test results of constant current for a smaller capacity battery cell.

Figs. 22 and 24 show that the average battery voltage difference for the optimal and the set time constant are 0.04 V and 0.15 V respectively, the corresponding variance are 0.74 and 0.79. In other words, fixing the time constant to a numeric value, satisfactory results can also be achieved.

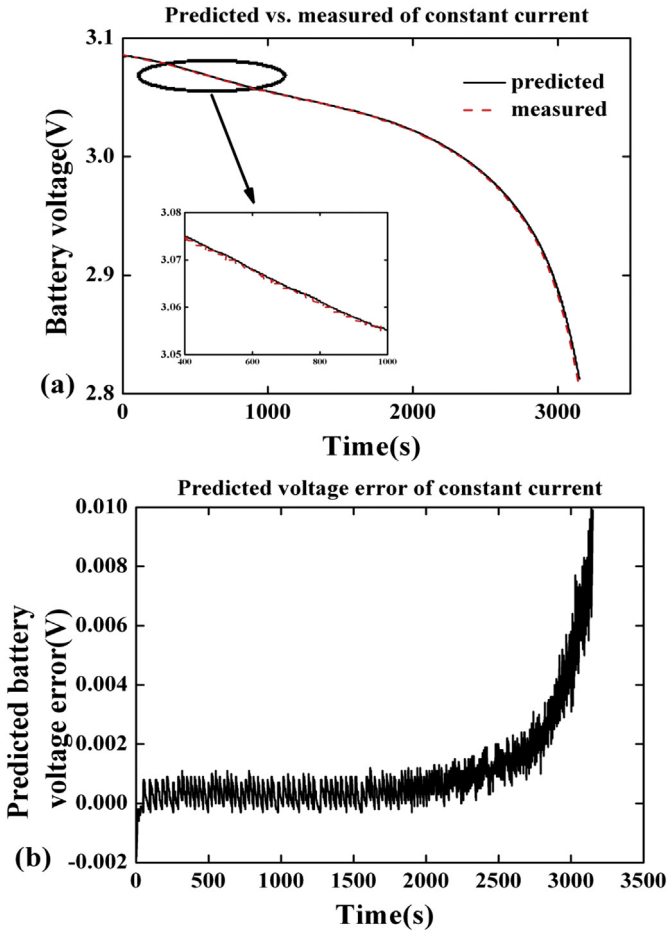

Fig. 19. (a) Results of measured and predicted with different time sizes of constant current for a smaller capacity battery cell and (b) predicted voltage error of constant current for a smaller capacity battery cell.

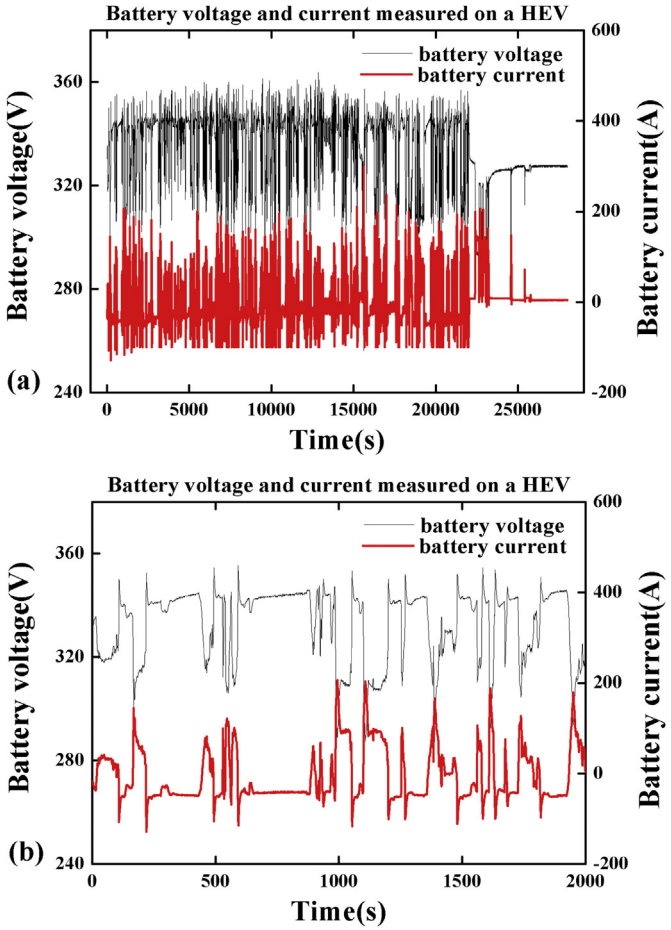

Fig. 20. Battery voltage and current measured with different time sizes on a HEV.

5. Conclusions

In this paper, a method that linearizes RC equivalent circuit models according to the 'DMC identification and prediction' algorithm has been proposed, the parameters of the linearized model could be dynamically identified by the least squares computation. The new method takes advantage of a feature of original DMC algorithm to predict battery available power. This method differs from the previous works in the literature in that the 'DMC identification and prediction' algorithm is introduced to identify the model parameters and predict battery state. The basic principles of this algorithm have been introduced, and the method has been validated by results of a bench test with lithium-ion battery cell (3.65 V, 100 Ah and 3.65 V, 10 Ah) and a HEV test with lithium-ion battery packs (320 V, 66 Ah) respectively in this paper.

The bench test results showed that the influence of long time constant RC blocks were not significant when current change drastically. The range of time constant of RC blocks were evaluated by means of statistical analysis of the testing conditions, and the time constants were selected to be at 10–50 s and 150–250 s for a second RC block. The second RC block and the first RC block equivalent circuit model were compared according to the model parameters identification and the battery voltage prediction. The results indicated that both models had the basically same accuracy under testing conditions. This supposes that the first RC block equivalent circuit could be used to describe the dynamic and steady state characteristics of a battery. But long time constants are required to describe the effect of concentration polarization. There

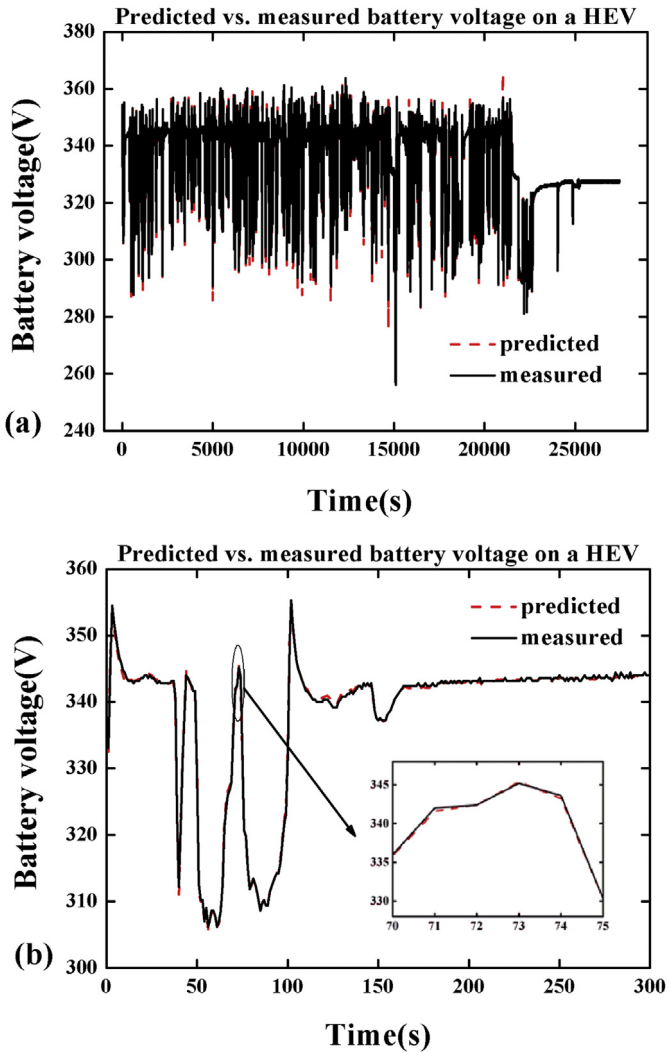

Fig. 21. Results of measured and predicted with different time sizes by the optimal time constant for a HEV based on improved DMC algorithm.

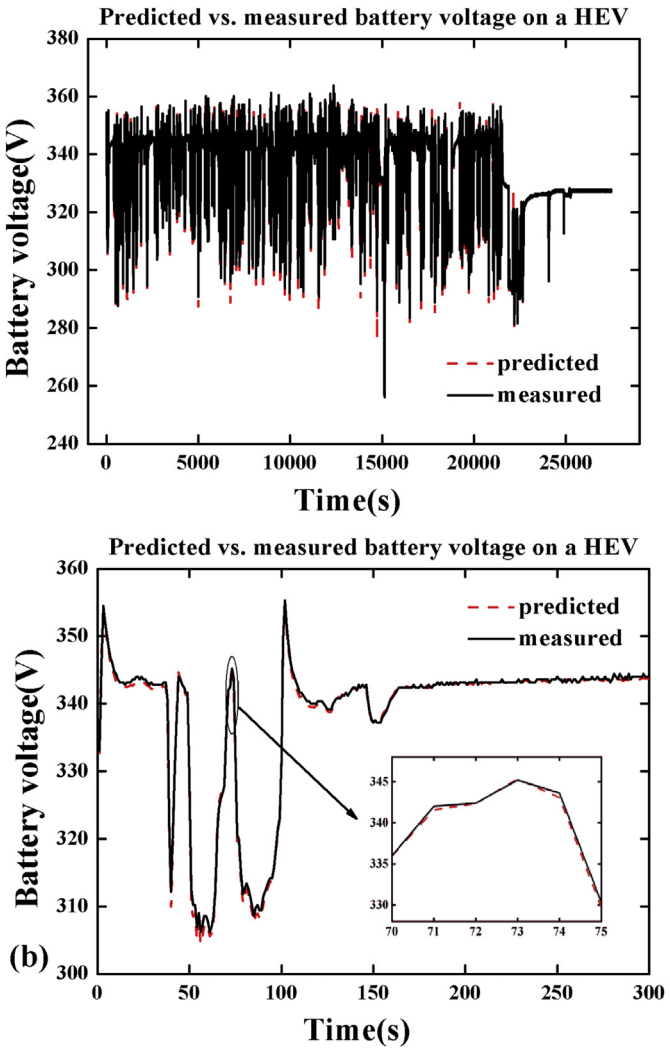

Fig. 23. Results of measured and predicted with different time sizes by the set time constant for a HEV based on improved DMC algorithm.

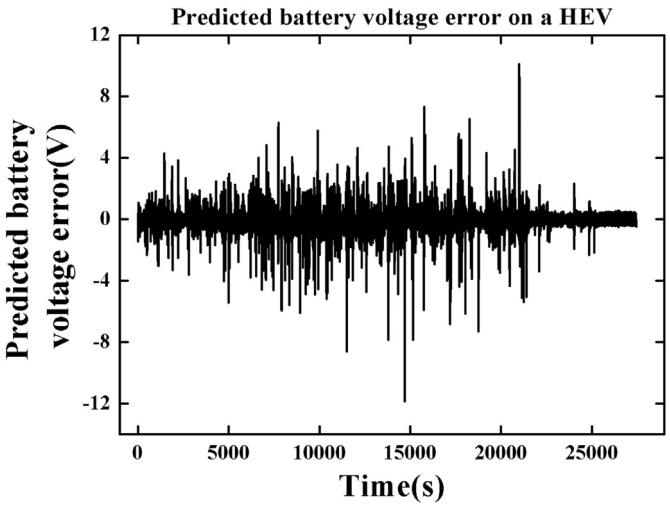

Fig. 22. Results of predicted voltage error by the optimal time constant for a HEV based on improved DMC algorithm.

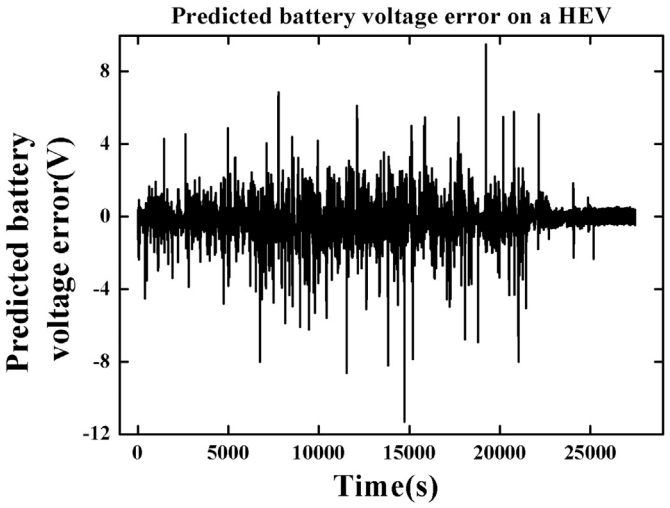

Fig. 24. Results of predicted voltage error by the set time constant for a HEV based on improved DMC algorithm.

was a difference between the identified open circuit voltage with that measured at battery rest stage for the first RC block equivalent circuit. According to the identified model parameters and the end of discharge voltage value, the battery available power at a future time could be predicted.

The HEV testing results showed that the battery voltage predicted by 'DMC identification and prediction' algorithm was also in good agreement with that measured, the maximum difference was within 3.7%. The comparison of using an optimal or a set time constant indicated that a set time constant would give similar results.

In the next step, the implementation of the algorithms on a BMS should be evaluated in terms of computation and accuracy for actual vehicle data.

References

[1] Y. Hu, Control Eng. Pract. 17 (2009) 1190–1201.
[2] G.L. Plett, J. Power Sources 134 (2004) 252–261.
[3] L.G. Lu, J. Power Sources 226 (2013) 272–288.
[4] V. Pop, H.J. Bergveld, et al., J. Electrochem. Soc. 153 (2006) 2013–2022.
[5] Amir Vasebi, J. Power Sources 174 (2007) 30–40.
[6] Jaemoon Lee, J. Power Sources 174 (2007) 9–15.
[7] Il-Song Kim, J. Power Sources 163 (2006) 584–590.
[8] G.L. Plett, J. Power Sources 134 (2004) 262–276.
[9] Y.J. Xing, Microelectron. Reliab. 53 (2013) 811–820.
[10] E. Barsoukov, J.R. Macdonald, Impedance Spectroscopy Theory, Experiment, and Applications, second ed., John Wiely & Sons, 2005.
[11] J.R.G. Guajardo, Accurate State of Charge Determination for Lithium–Iron Phosphate Battery Packs, November 2011.
[12] G.L. Plett, J. Power Sources 134 (2004) 277–292.
[13] C. Li, Study on Parameter Identification and SOC Estimation of Ni/MH Battery for EV (Master dissertation), Tianjin University, June 2007.
[14] Y. Hu, J. Power Sources 196 (2011) 2913–2923.
[15] R.D. Kokate, Int. J. Control Automation 4 (2011) 95–110.
[16] V.H. Johnson, J. Power Sources 110 (2002) 321–329.
[17] C.T. Lin, B. Qiu, Q.S. Chen, Automot. Eng. 28 (2006) 38–42.
[18] J. Thevenin, J. Power Sources 14 (1985) 45–52.
[19] U.S. Dept of Energy, FreedomCAR Battery Test Manual for Power-Assist Hybrid Electric Vehicles, DOE/ID-11069, 2003.
[20] Tarun Huria, in: 2012 IEEE International Electric Vehicle Conference (IECV), IEEE, Greenville, SC, USA, 2012, pp. 1–8.
[21] Z. Li, Characterization Research of $LiFePO_4$ Batteries for Application on Pure Electric Vehicles (Doctoral dissertation), Tsinghua University, April 2011.
[22] U.S. Dept of Energy, PNGV Battery Test Manual, Revision 3, DOE/ID-10597, 2001.